

Bulk-Silicon Resonant Accelerometer *

Jia Yubin¹, Hao Yilong¹, and Zhang Rong²

(1 Institute of Microelectronics, Peking University, Beijing 100871, China)

(2 Department of Precision Measurement Technology and Instrument, Tsinghua University, Beijing 100084, China)

Abstract : Resonant accelerometer is designed, which includes two double-ended tuning forks, a proof mass, four-leverage system amplifying inertial force, and drive/sense combs. Each tuning fork is electrostatically actuated and sensed at resonance using comb electrodes. The device is fabricated using MEMS bulk-silicon technology, whose sensitive degree is 27.3 Hz/g, and the resolution is 167.8 μ g.

Key words : MEMS accelerometer; resonant driving and sensing; bulk-silicon process; frequency shift

EEACC : 2520C; 2560F

CLC number : TN304.12

Document code : A

Article ID : 0253-4177(2005)02-0281-06

1 Introduction

Accelerometers are used for diverse areas ranging from inertial navigation to vibration monitoring. Micromachined accelerometers are widely used for automotive industry because of their low cost, small size, and broad frequency response^[1]. Various accelerometers based on a number of different techniques and principles^[2~7] have been designed and implemented. In the majority, the acceleration to be measured is converted into a displacement of movable proof mass. This displacement can be picked up by optical, capacitive, piezoresistive or tunneling methods^[4~7]. However, the resonant accelerometers are operated by detecting frequency shift due to the inertial force which is caused by the applied acceleration in the resonant characteristics of the devices. For a direct frequency output, resonant sensors have many advantages over

conventional type such as high resolution, wide dynamic range, quasi-digital nature, and the inherent continuous self-test capability^[8]. The quartz-based resonant accelerometers have been used for navigation-grade sensing^[9]. During last few years, basing on resonant principle, several resonant accelerometers have been reported, including surface^[10,11], bulk^[12], and mixed (bulk and surface)^[8] micromachining process. In 1997, Roessig *et al.* designed and fabricated a DETF (double-ended tuning fork) resonant accelerometer with a 45 Hz/g scale factor using a lever system to magnify the inertial force applied to the tuning fork^[10]. In 2002, Seshia *et al.* improved lever structure and fabricated a DETF accelerometer with a 17 Hz/g scale factor and a noise floor of 40 μ g/Hz^{1/2} for input accelerometer frequency of 300 Hz^[11].

Resonant sensor monitors the measurand as a function of resonant frequency of the vibrating structure or resonator. A key determinant of the perfor-

* Project supported by National High Technology Research and Development Program of China (No. 2002AA430020)

Jia Yubin male, was born in 1964, associate professor. His main research interests include MEMS, MOEMS, and integrated optics. Email: ybjia@ime.pku.edu.cn

Hao Yilong male, was born in 1963, professor. His research interests include MEMS and its new devices and new processes.

Zhang Rong male, was born in 1968, associate professor. His research interests include micromachined gyroscope and accelerometer.

Received 23 June 2004, revised manuscript received 16 September 2004

© 2005 Chinese Institute of Electronics

mance of the device is the amount of energy coupled through the resonator's supports to the surroundings. The level of coupling can be reduced by designing a dynamically balanced resonator. DETF resonator mentioned above is the simplest form of stress sensitive dynamically balanced structure^[10,11]. In order to elevate the sensitivity and stability of resonant accelerometer, improving the structure of resonant accelerometer is essential. We design and fabricate a resonant accelerometer with a 27.3 Hz/g scale factor and a 167.8 μg resolution using bulk-silicon process.

2 Structure description

The structure of the resonant accelerometer is shown in Fig. 1. This accelerometer consists of two double-ended tuning forks, a proof mass surrounding two tuning forks and extending around, four leverage systems, and drive/sense combs.

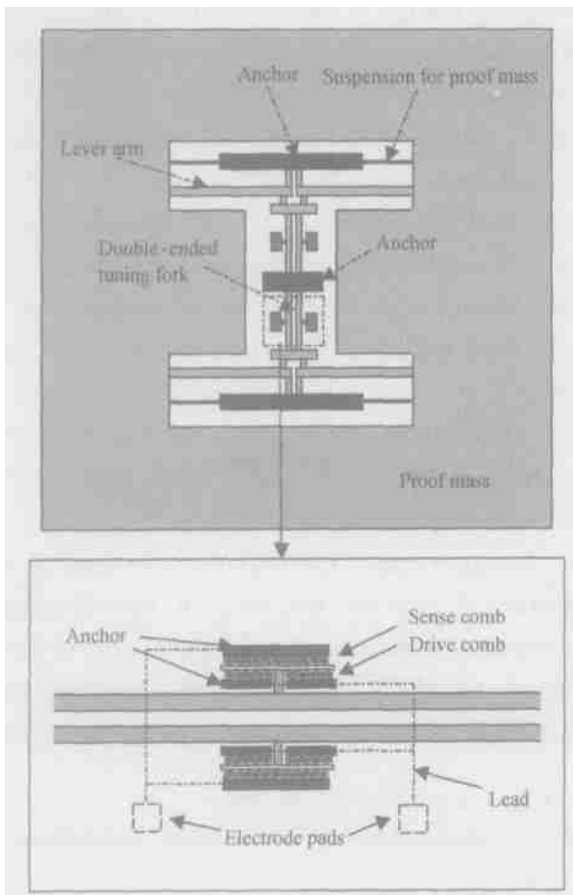


Fig. 1 Structure of the resonant accelerometer

The proof mass is attached to two double-ended tuning fork resonators via four mechanical-leverage arms. In order to maximize the scale factor, the four leverage systems are used to magnify the inertial force applied to the tuning forks. Each tuning fork is electrostatically actuated and sensed at resonance using comb electrodes. When an external acceleration is applied to the device, one tuning fork is subjected to a tensile force which raises its natural frequency, and the other tuning fork experiences a compressive force, lowering its frequency. Two double-ended tuning forks provide for a differential output which is twice sensitivity of the one double-ended tuning fork and avoid or lower the ambient noise.

3 Frequency shift due to acceleration

The natural frequency of a clamped-clamped beam subjected to a concentrated load (combs) that is applied to the center of the beam in its primary mode of the operation is given by

$$f_0 = \frac{7.044}{\sqrt{12}} \times \sqrt{\frac{E}{\rho}} \times \left(\frac{w}{l}\right)^3 \times \frac{1}{(s + 0.3965 w l)} \quad (1)$$

where ρ is the material density, E is the Young's modulus, l and w is the length and thickness of the beam, respectively, s is the total surface area of the movable combs.

The change of the natural frequency as a function of applied axial force is^[13]

$$f = f_0 (1 \pm Fp)^{\frac{1}{2}} \quad (2)$$

where $p = 0.2949 \times \frac{l^2}{Ew^3 h}$, $F = Cma = CSha$, C is the lever amplification factor, S and h are the total area and thickness of the proof mass, respectively, a is the applied acceleration.

Note that the positive sign “+” is changed into the negative one “-” in Eq. (2) if the compressive force is applied on the double end of the sense beam.

Since there are two equally matched tines for DETF, the axial force caused by the applied acceleration on each tine is halved as compared to the case for a single clamped beam. Because the frequency shift

f is small as compared to the center frequency f_0 and there are two equally matched DETFs in Fig. 1 , the relative frequency shift of the structure designed in Fig. 1 is written as

$$\frac{-f}{f_0} \approx \frac{1}{8} Fp \tag{3}$$

Using the differential output $f = f_1 - f_2$, and $f_1 = -f_2$, the scale of the device can be expressed as

$$\frac{-f}{a} = \frac{2-f}{a} = 0.07372 C S \frac{l^2 f_0}{Ew^3} \tag{4}$$

Table 1 is a list of the implemented design parameters of the resonant accelerometer.

Table 1 Design parameters

Parameter	Symbol	Design value
DETF tine length	l	800 μ m
DETF beam width	w	5 μ m
DETF natural frequency	f_0	24.9kHz
Proof mass area	S	4.6 $\times 10^6 \mu$ m ²
Thickness of the proof mass and comb fingers and tuning forks	h	80 μ m
Total area of the movable combs	S	1.2 $\times 10^4 \mu$ m ²
Number of sensing comb finger	N_s	53
Number of driving comb finger	N_d	46
Comb finger gap	d	3 μ m
Finger motion range	X_0	7.5 μ m
Comb finger length	l_c	25 μ m
Lever amplification	C	20
Scale factor	f/a	113Hz

4 Fabrication process

The standard bulk-silicon micromachining technology is used to manufacture the resonant accelerometer (Fig. 1) ,which combines ICP deep etching with Si-glass bonding technology. The fabricating process of the resonant accelerometer involves three-time photolithography, and its advantages refer to simplicity and high reliability ,etc. The basic steps of fabrication are as follows :

Firstly the double sides of the silicon wafer were oxidized thermally ,then the first photolithography

was done in the one face :using the positive photoresist as the mask and the useless silicon dioxide was taken out by the reactive ion etching (RIE) ,then removing photoresist and using silicon dioxide as the mask ,the silicon on the surface was etched with KOH solution ,and the protruded parts about 5 μ m high as the anchors of the fixed combs and the suspension of the proof mass and tuning forks were generated as shown in Fig. 2 (a) . At the same time ,the second photolithography was done in the surface of the glass. The shallow trenches were patterned and etched. A Ti-Pt-Au layer of about 200nm was sputtered on Pyrex glass wafer ,followed by lift-off patterning to form the electrodes and leads as shown in Fig. 2(b) .

The silicon dioxide on the inverse face was protected by gelatinizing photoresist ,then the silicon dioxide on the former face was etched by HF solution. After the photoresist on the inverse face was taken out ,a heavy B⁺ surface doping was done to get well ohmic contact. Finally the silicon dioxide on the inverse face was etched out. The silicon wafer was inverted and bonded with Pyrex glass wafer ,and therefore the protrudent parts were fixed on the glass and were combined with the leads. Then the silicon wafer was thinned with KOH solution to 50 ~ 80 μ m thickness ,which was the structure layer of the accelerometer as shown in Fig. 2(c) .

The Al membrane was sputtered on silicon wafer. The third photolithography was done using the photoresist as the mask ,and the pattern of the accelerometer appeared. Using Al as the mask ,the silicon wafer was etched to the glass by ICP method ,so the moveable structure of the accelerometer was released as shown in Fig. 2(d) .

Using digital camera under 20 \times magnification microscope ,we took two photographs of above fabricated structure as shown in Fig. 3. This structure bears equally matched tuning forks in the center. The right in Fig. 3 (b) is electrode pads which are connected with drive and sense circuits.

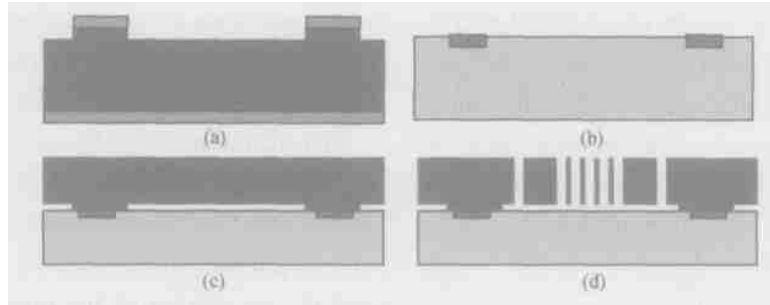


Fig. 2 Fabricating process of the resonant accelerometer

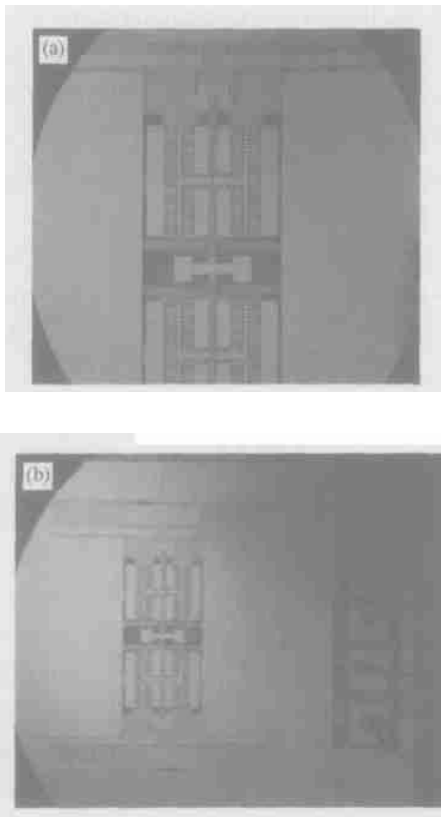


Fig. 3 Micrograph of the fabricated structure of the resonant accelerometer

5 Measurement results

Using the swivel table and Agilent 53131 all-purpose arithmometer, some parameters of the fabricated sample of the accelerometer were measured such as sensitivity and resolution.

First the sample was fixed parallel on the swivel table, and the output signal of the accelerometer was connected to the arithmometer. Turning the swivel table and looking for the maximal and minimal value of the output signal, signing the corresponding position which was defined as $\pm 1g$, and defining the zero-output position in middle between two positions as reference mark of the zero position, the points spacing 10° from $-90^\circ (-1g)$ to $+90^\circ (+1g)$ were measured for 20s and noted. We adopted the average of the output values for 20s as the measured value of the point and noted it. The measured data are shown in Table 2. These data were fitted by linearity as shown in Fig. 4. Then the sensitivity of the accelerometer was obtained.

Table 2 Measured data of the accelerometer

Angle/ ($^\circ$)	- 90	- 80	- 70	- 60	- 50	- 40	- 30	- 20	- 10	0
Output value/ Hz	1328.50	1328.94	1330.19	1332.39	1335.38	1339.07	1343.29	1348.13	1352.87	1357.14
Angle/ ($^\circ$)	90	80	70	60	50	40	30	20	10	
Output value/ Hz	1383.11	1382.79	1381.77	1379.67	1377.15	1373.84	1370.23	1366.11	1361.64	

Setting the accelerometer on zero position, connecting the output signal of the accelerometer to the arithmometer, setting the operation mode of the arithmometer on the square-difference statistic mode, and

noting the square-difference value of the accelerometer, the resolution of the accelerometer was obtained by a ratio of the square-difference value to the sensitivity.

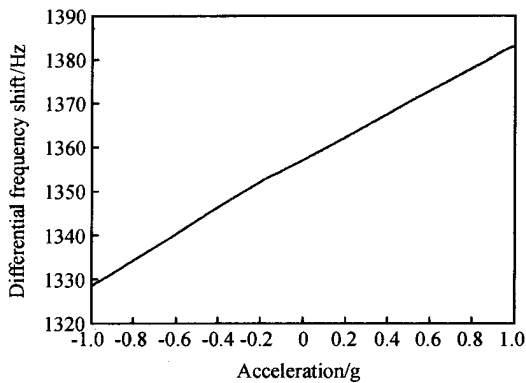


Fig. 4 Linear fitted curve of the testing data of the accelerometer

According to above experimental data, the sensitivity of the accelerometer sample is 27.3 Hz/g , the resolution is $0.00458/27.3 = 167.8 \mu\text{g}$, and the resonant frequency is around 25 kHz which agrees with calculating result. The measured sensitivity of the device is around a quarter of the calculating result because the lever amplification is not up to 20 due to the flexure of lever arm and suspension for proof mass, and in fact the lever amplification is only $4 \sim 5$. By improving the structure size of the lever, the amplification may be upwards of 10.

6 Conclusion

The structure of a resonant accelerometer is presented, which includes two doubly clamped tuning forks, a proof mass surrounding two tuning forks and extending around, four-lever system amplifying inertial force, and drive/sense combs. The force acting on the axis of the tuning forks due to applied acceleration raises the frequency due to a tensile force for one fork, and at the same time lowers the frequency due to compressive for the other fork. Each tuning fork is electrostatically actuated and sensed at resonance using comb electrodes. Two double-ended tuning forks provide for a differential output which is twice sensitivity of the one double-ended tuning fork and avoid or lower the ambient noise. The device has been fabri-

cated using MEMS bulk-silicon technology. The sensitive degree of the accelerometer sample is 27.3 Hz/g , and the resolution is $167.8 \mu\text{g}$.

References

- [1] Yazdi N, Ayazi F, Najafi K. Micromachined inertial sensors. Proc IEEE, 1998, 86:1640
- [2] Li Lijie, Liang Chunguang. Micromachined thermal convection accelerometer. Chinese Journal of Semiconductors, 2001, 22(4): 465 (in Chinese) [李立杰, 梁春广. 微机械热对流加速度计. 半导体学报, 2001, 22(4):465]
- [3] Zhou Jun, Wang Xiaohong, Yao Pengjun, et al. Analysis and design of an accelerometer fabricated with porous silicon as sacrificial layer. Chinese Journal of Semiconductors, 2003, 24(7):687
- [4] Larsen T S, Bouwstra S, Leistiko O. Opto-mechanical accelerometer based on strain sensing by a Bragg grating in a planar waveguide. Transducer, 1995:667
- [5] Chau K H, Lewis S R, Zhao Y, et al. An integrated force-balanced capacitive accelerometer for low-g application. Transducers, 1995:539
- [6] Chen H, Bao M, Zhu H, et al. A piezoresistive accelerometer with novel vertical beam structure. Transducer, 1997:1201
- [7] Liu C H, Barzilai A M, Reynolds J K, et al. Characterization of a high-sensitivity micromachined tunneling accelerometer with micro-g resolution. J Microelectromech Syst, 1998, 7(2):235
- [8] Seok S, Seong S, Lee B, et al. A high performance mixed micromachined differential resonant accelerometer. Proc IEEE, 2002, 2(12~14):1058
- [9] Norling B L. Superflex: a synergistic combination of vibrating beam and quartz flexure accelerometer. Journal of Navigation, 1988, 34(4):337
- [10] Roessig T, Howe R, Pisano A, et al. Surface-micromachined resonant accelerometer. Proc Ninth International Conference on Solid-State Sensors and Actuators, Transducers, Chicago, 1997:859
- [11] Seshia A A, Palaniapan M, Roessig T A, et al. A vacuum packaged surface micromachined resonant accelerometer. J Microelectromech Syst, 2002, 11(6):784
- [12] Burrer C, Esteve J, Lora-Tamayo E. Resonant silicon accelerometers in bulk micromachining technology-an approach. J Microelectromech Syst, 1996, 5(2):122
- [13] Jia Yubin, Hao Yilong, Zhong Ying, et al. Micromachined accelerometer based on resonant principle. Micronanoelectronic Technology, 2003, 40(7/8):271 (in Chinese) [贾玉斌, 郝一龙, 钟莹, 等. 基于谐振原理的硅微机械加速度计. 微纳电子技术, 2003, 40(7/8):271]

一种新型体硅谐振加速度计^{*}

贾玉斌¹ 郝一龙¹ 张 嵘²

(1 北京大学微电子研究所, 北京 100871)

(2 清华大学精密仪器系, 北京 100084)

摘要: 设计了一种谐振加速度计. 这种加速度计包括两个双端固定音叉、一个质量块、四套放大惯性力的杠杆系统以及激励和敏感梳. 利用梳状电极每个音叉被静电激励和敏感. 利用 MEMS 体硅工艺研制了这种新型加速度计, 测试的灵敏度为 27.3 Hz/g, 分辨率为 167.8 μ g.

关键词: MEMS 加速度计; 谐振激励和敏感; 体硅工艺; 频率漂移

EEACC: 2520C; 2560F

中图分类号: TN304.12

文献标识码: A

文章编号: 0253-4177(2005)02-0281-06

^{*} 国家高技术研究发展计划资助项目(批准号:2002AA430020)

贾玉斌 男,1964 年出生,副教授,从事 MEMS 及 MOEMS 和集成光学方面的研究. Email:ybjia@ime.pku.edu.cn

郝一龙 男,1963 年出生,教授,从事 MEMS 及其新器件和新工艺方面的研究.

张 嵘 男,1968 年出生,副教授,从事微陀螺和加速度计的研究.

2004-06-23 收到,2004-09-16 定稿